PHYSICAL REVIEW B **77**, 245414 (2008)

Reconstructions on the polar $SrTiO_3$ (110) surface: Analysis using STM, LEED, and AES

Bruce C. Russell and Martin R. Castell*
Department of Materials, University of Oxford, Parks Road, Oxford OX1 3PH, United Kingdom
(Received 17 January 2008; published 10 June 2008)

Scanning tunneling microscopy, Auger electron spectroscopy (AES), and low energy electron diffraction are used to investigate 0.5 wt % Nb doped $SrTiO_3$ (110) samples, which are annealed in ultrahigh vacuum. An $(n\times1)$ family of reconstructions constituting (3×1), (4×1), and (6×1) periodicities form on the surface at varying annealing temperatures. Wood's notation of the reconstructions is defined such that the first integer represents the multiple of the bulk terminated periodicity in the [001] direction and the second digit shows the multiple of the periodicity in the $[1\bar{1}0]$ direction. AES reveals that all the reconstructions are O deficient, but the (4×1) is also Ti enriched and the (6×1) is Sr enriched with respect to stoichiometry. The (3×1) surface possesses step edges which are decorated with a (1×4) reconstruction on the upper terrace. Similarly, step edges on the (6×1) surface often possess small regions of (1×2) reconstruction on the lower terrace. Step heights are always found to be equivalent to integer multiples of the distance between two similar {110} planes (the d_{110} lattice parameter, 0.28 nm).

DOI: 10.1103/PhysRevB.77.245414 PACS number(s): 68.47.Gh, 68.37.Ef, 61.05.jh, 79.20.Fv

I. INTRODUCTION

The surfaces of complex metal oxides are of interest because the presence of two (or more) species of cations allows nonstoichiometry in the surface region to act as a surface stabilization mechanism. Simple metal oxides tend to have a fixed concentration of the metal cations relative to the oxygen anions, which means that the chemical composition of the surface remains relatively constant. An exception to this is where cations of multiple valency are involved such as titanium. Complex metal oxides only need to maintain electrical neutrality between all the metal cations and oxygen anions, which means that the concentration of one metal can increase relative to another as long as the overall charge remains zero. A change in the surface stoichiometry is a mechanism that may lower the surface energy. It is possible that a number of stoichiometries have energies low enough to form stable surface phases, leading to a number of different surface reconstructions.

Strontium titanate is a perovskite oxide with formula $SrTiO_3$. Figure 1(a) shows the unit cell of $SrTiO_3$, which is cubic with a lattice parameter of 0.3905 nm. Ti ions sit on the corners of the unit cell with O ions in the center of each vertex and a Sr atom at the center of the unit cell. Much work has been done on $SrTiO_3$ (001) with both Ti (Refs. 1–7) and Sr (Refs. 8–10) rich phases being observed on the surface after different preparation methods. The other low Miller index polar surfaces have been less extensively studied. Polar surfaces are those whose bulk terminated surface would have a macroscopic dipole perpendicular to it. This is caused by the alternating stacking of equally but oppositely charged positive and negative atomic layers within the bulk of the material, parallel to the surface of interest. If this dipole were to exist, it would cause the energy of the surface to be infinite[11] (on the assumption of a semi-infinite crystal, which is a close approximation to a macroscopic crystal). The bulk terminated surface of a polar termination can therefore not exist, and the surface must change in some way in order to redistribute its charge and neutralize the dipole.[12] The surface will always respond using various mechanisms in order to prevent the dipole from occurring and to lower its energy.[13] Both the $SrTiO_3$ (111) and (110) terminations are polar. We have previously found $SrTiO_3$ (111) to produce reconstructions that are Ti enriched.[14,15]

The $SrTiO_3$ (110) surface is polar because it is made up of alternating $SrTiO^{4+}$ and O_2^{4-} layers.[16] Figure 1(a) shows the position of the (110) plane, indicated in gray, in the $SrTiO_3$ bulk unit cell. Figure 1(b) is a schematic of a (110) terminated crystal viewed from the side so that the alternating $SrTiO^{4+}$ and O_2^{4-} layers can be seen. On the left, the crystal is terminated by an O_2^{4-} plane, and on the right by a $SrTiO^{4+}$ plane. Figure 1(c) shows the (1×1) surface unit cell of the $SrTiO_3$ (110) termination. Unlike the (100) and (111) surfaces, the (110) surface possesses an anisotropic unit cell, as the main crystallographic unit cell dimensions along the [001] and $[1\bar{1}0]$ directions have different lengths. Reconstructions on the (110) surface are defined in Wood's notation with the first digit representing the [001] direction and the second the $[1\bar{1}0]$ direction. As an example, the difference between a (1×3) and a (3×1) reconstruction is illustrated in Fig. 1(c).

The work completed so far on the $SrTiO_3$ (110) surface is sparse and somewhat contradictory. The main study to date was produced by Brunen and Zegenhagen[17] who used scanning tunneling microscopy (STM), low energy electron diffraction (LEED), and Auger electron spectroscopy (AES). They reported that the Sr concentration increased with increasing anneal temperature. Annealing in ultrahigh vacuum (UHV) at different temperatures and annealing times produced (2×5), (3×4), (6×6), and (4×4) reconstructions. STM images of (2×5) and (4×4) showed two different morphologies. Annealing an Ar^+ ion sputtered sample gave a (6×4) surface with a strong ridge structure, which followed the $[1\bar{1}0]$ direction. All the surfaces produced LEED patterns with missing spots and STM images with little atomic detail and could be interpreted as different coexisting reconstructions.

Bando *et al.*[18] observed a metallic $SrTiO_3$ (110) reconstruction in STM, with approximate (5×2) periodicity, after

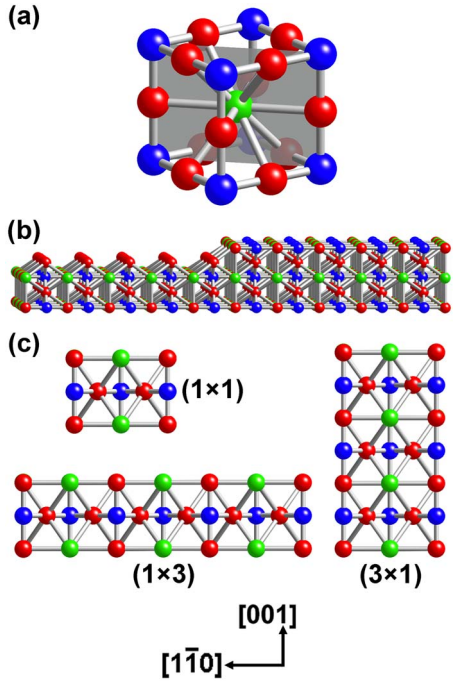

FIG. 1. (Color online) Schematic representations of the $SrTiO_3$ (110) surface. The Sr atoms are green (light gray), the O atoms are red (dark gray), and the Ti atoms are blue (black). (a) The bulk unit cell of $SrTiO_3$ with the (110) plane indicated in gray. (b) A side view of the $SrTiO_3$ (110) surface showing the alternating $SrTiO^{4+}$ and O_2^{4-} planes. The terminating plane on the right is $SrTiO^{4+}$ and that on the left is O_2^{4-}. A quarter unit cell height ($0.5\,d_{111}$ =0.14 nm) step edge is shown separating the two. (c) The $SrTiO_3$ (110) surface viewed from above. The (1×1) unit cell is shown. The anisotropy of the crystallographic directions is indicated by the difference between the (1×3) and (3×1) unit cells.

an 800 °C anneal for 3 h in UHV. Annealing at 1100–1200 °C produced an insulating surface with approximately (4×2) or (5×2) periodicity. In addition, repeated anneals at 1200 °C produced a $c(2\times6)$ reconstruction, which was modeled to include the existence of Ti^{3+} and Ti^{2+} ions.

Gunhold *et al.*[19,20] have found that microfaceting is also possible on the surface. Samples were annealed at 900 °C in 1 atm air and at 1000 °C in UHV. Both contained faceting with a (1×1) and (1×2) periodicity. The (1×1) was also observed by Brunen *et al.*[17] These can be formed by the removal of Sr from the top two surface layers. This was supported by AES and the agreement of Hartree–Fock calculations and metastable impact electron spectroscopy.

There are a large number of $SrTiO_3$ (110) reconstructions, which have all been reported by different groups and which form under similar conditions. In this paper, we hope to bring some clarity to this situation by using a combination of STM, LEED, and AES to characterize the reconstructions of the $SrTiO_3$ (110) surface.

II. EXPERIMENT

Single crystals of $SrTiO_3$ doped with Nb at 0.5% by weight with epipolished (110) surfaces were supplied by PIKEM, UK. As $SrTiO_3$ is an insulator with a band gap of 3.2 eV at 25 °C,[21] the addition of Nb dopes $SrTiO_3$ *n*-type, giving rise to sufficient electrical conductivity at room temperature for STM experiments to be performed. The crystals were cut to size and then introduced without pretreatment into the UHV chambers of two instruments. These were a JEOL JSTM4500xt, which includes STM and LEED analysis facilities, and a JEOL JSTM4500s comprising STM, LEED, and a UHV scanning electron microscope (SEM) with a SPECS PHOIBOS 100 electron energy analyzer. The UHV SEM and electron energy analyzer were used in combination to provide AES at high spatial resolution. LEED patterns were produced by using a four mesh VG Microtech rear view system and captured with a Cannon SLR digital camera. The vacuum pressure in each instrument was regularly observed to be of the order of 10^{-8} Pa. Constant current STM images were produced at room temperature by using etched tungsten tips. The samples were annealed by resistively passing a direct current through the sample and the temperatures were measured through a viewport with an optical pyrometer.

III. RESULTS

A. (3×1) reconstruction

When a sample is introduced to the vacuum chamber and annealed at 875 °C for 2 h and analyzed by using the STM, images like those in Fig. 2 are produced. Figure 2(a) shows a large scale scan of the resulting surface. The step edges are straight and follow the [001] and [1$\bar{1}$0] crystallographic directions. Step heights are 0.27 ± 0.03 nm. In addition, there are two distinct regions visible in the images. The region labeled α covers most of the image. It is made up of stripes all following the [1$\bar{1}$0] direction. These stripes also have defects at certain points where there appears to be a slightly larger than usual gap between the lines that make up the reconstruction. One such defect is indicated by a white arrow in Fig. 2(a). In addition to this region, there is also another structure present. These regions (labeled β) occur at the step edges, as raised islands above the α region, and occasionally sit within the α region itself. Although on initial inspection the β regions look somewhat disordered, on closer inspection, they contain stripes within them which follow the [001] direction. The β regions are hard to image and appear structurally unresolved across all STM bias voltages. Most [001] step edges occur with a domain of β reconstruction occurring along them. One of the β regions is shown in detail in Fig. 2(b). This shows a small β island, which is surrounded by step edges. It was difficult to image this region but information about its periodicity can be obtained. The periodicity of the reconstruction in the [001] direction is shown in the line scan of Fig. 2(d) and is measured to be 0.38 ± 0.03 nm, which corresponds to the bulk periodicity in that direction. Figure 2(e) shows a line scan with the periodicity in the [1$\bar{1}$0] direction, which is 2.14 ± 0.09 nm and is equivalent to four times the bulk periodicity. There does, however, seem to be some disorder to the surface. This may be due to defects or adsorbates (possibly water or hydrogen from the residual atmosphere) sitting on top of the surface. This may also be

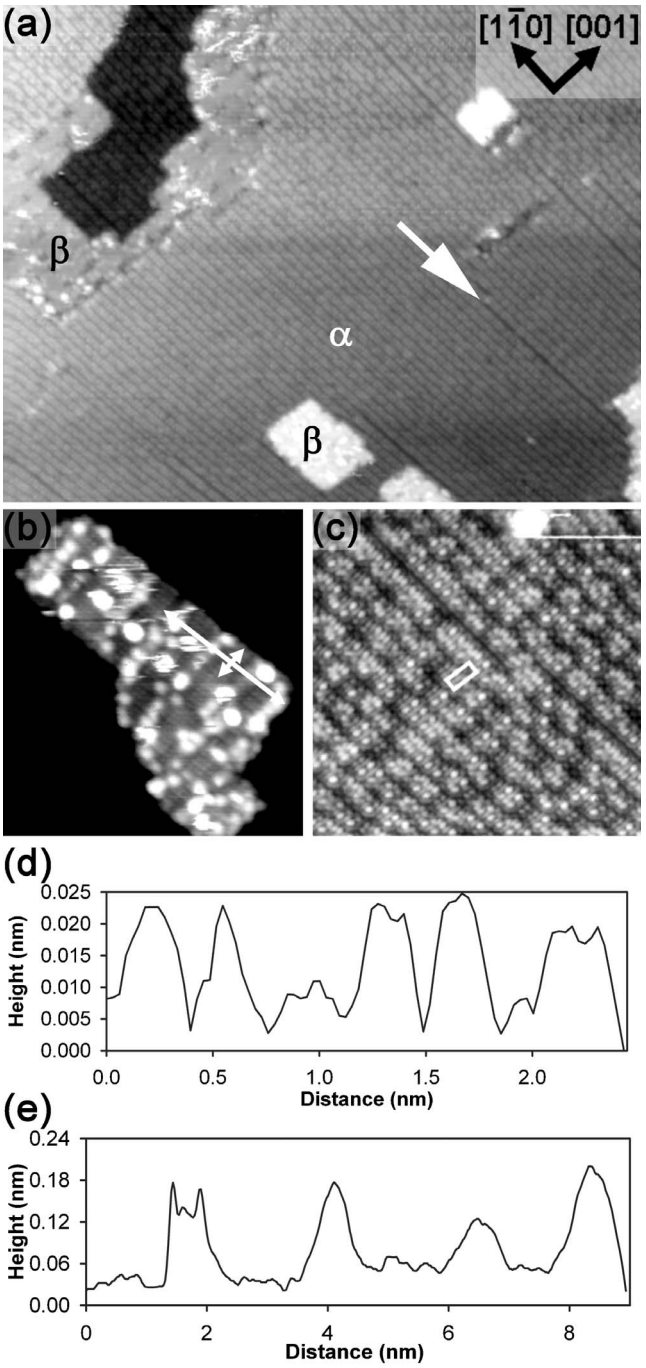

FIG. 2. STM images of the (3×1) and (1×4) reconstructions of $SrTiO_3$ (110). (a) A terrace comprised mostly of (3×1) reconstruction. The striped region, labeled α, oriented along the $[1\bar{1}0]$ direction is the (3×1) reconstruction. The step edges are straight and follow the $[1\bar{1}0]$ and [001] directions. At the step edges and on top of the raised regions in the bottom, a different morphology is shown, labeled β. This is the (1×4) reconstruction, and it generally decorates the [001] step edges. A number of phase boundaries can be seen in the (3×1) reconstruction, and one is indicated by a white arrow (image size 68×54 nm^2, sample bias +0.8 V, and tunneling current 0.4 nA). (b) A region of (1×4) reconstruction, which constitutes a raised terrace. This is the same reconstruction, as represented by the β regions in Fig. 2(a). Although the reconstruction is difficult to image due to the bright spots that feature on it, both the $[1\bar{1}0]$ and [001] periodicities can be seen (image size 16×18 nm^2, sample bias +0.7 V, and tunneling current 0.2 nA). (c) A more detailed image of the (3×1) reconstruction. This is the same reconstruction as the region labeled α in Fig. 2(a). The stripes consist of double rows of bright spots. The (3×1) unit cell is indicated (image size 14×14 nm^2, sample bias +0.8 V, and tunneling current 0.4 nA). (d) Line scan for the shorter white double headed arrow in the [001] direction from part (b). The periodicity is equivalent to bulk periodicity in this direction (0.3905 nm). (e) Line scan for the longer white double headed arrow in the $[1\bar{1}0]$ direction from part (b). The periodicity is equivalent to four times the bulk periodicity in this direction (2.2 nm).

the factor that makes the (1×4) reconstruction difficult to image.

Region α is shown in detail in Fig. 2(c). Atomic detail of the stripes can be seen. The periodicity in the $[1\bar{1}0]$ direction is 0.52 ± 0.03 nm, which is equivalent to that of the underlying bulk unit cell, and that in the [001] direction is 1.12 ± 0.10 nm, which is equivalent to three times that of the underlying bulk unit cell, giving an overall (3×1) periodicity. The unit cell of the reconstruction is indicated by a white rectangle in the center of the image. The reconstruction also features a number of bright spots that appear at regular points but do not cover the entire surface. These may be due to defects or adsorbates from the residual atmosphere, but as they arrange in a more ordered way on the surface, they are less detrimental to the imaging of the reconstruction in the STM. The defects which cause the stripes to be separated by a larger gap are caused by a shift of the reconstruction by a single bulk unit cell in the [001] direction. This causes a gap of a single bulk unit cell to separate two (3×1) reconstructed stripes, as indicated by the white arrow in Fig. 2(a).

The periodicities measured by STM are confirmed by LEED. Figure 3(a) shows a (3×1) LEED pattern obtained for this surface. The spots of the (3×1) pattern are intense and all are clearly visible. In the figure, it is not possible to see the (1×4) spots. This is because the (1×4) makes up only a small proportion of the surface and, thus, its spots are much less intense than those of the (3×1) surface. Although the camera could not easily capture it, a few of the (1×4)

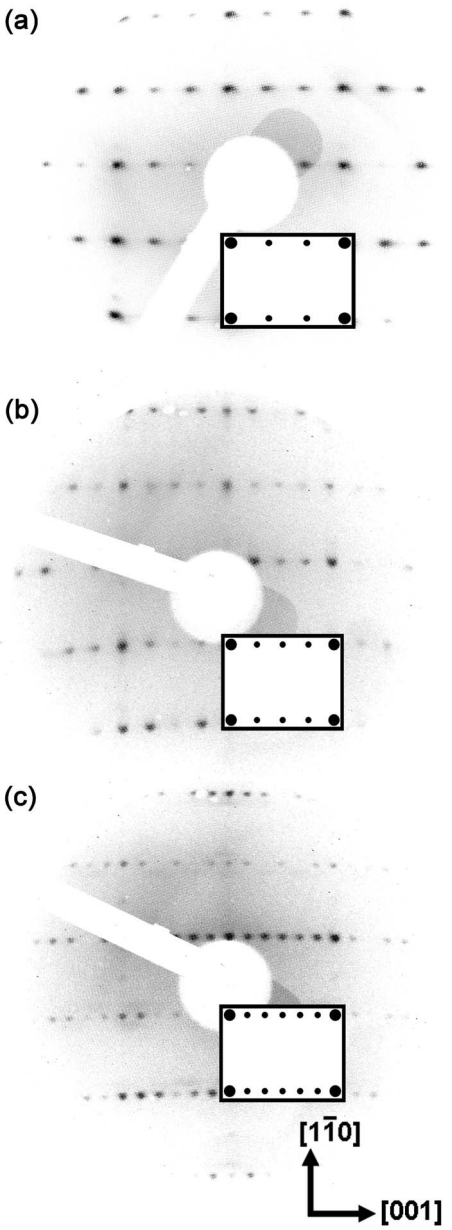

FIG. 3. LEED patterns for the $SrTiO_3$ (110) surfaces. All LEED patterns were taken at 60 eV. The computer generated LEED patterns in the boxes were obtained by using LEEDPAT (Ref. 25). (a) LEED pattern for the (3×1) surface. (b) LEED pattern for the (4×1) surface. (c) LEED pattern of the (6×1) surface.

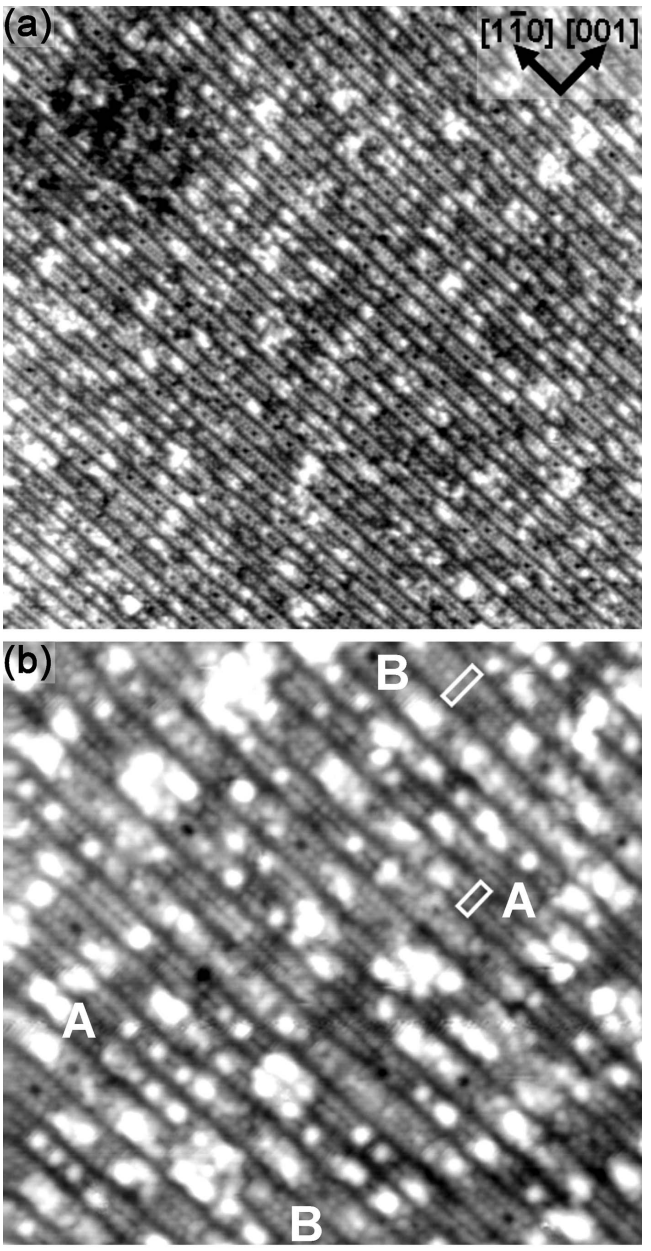

FIG. 4. (a) STM image showing ridges running in the $[1\bar{1}0]$ direction (image size 68×66 nm^2, sample bias +1.4 V, and tunneling current 0.05 nA). (b) A more detailed image of the surface. Wider and narrower stripes can be seen. Two wider stripes are labeled B and two narrower stripes are labeled A. The wider stripes consist of three rows of atoms and are associated with a (4×1) reconstruction. The narrower stripes consist of two atomic rows and are associated with a (3×1) reconstruction. The unit cells of the two types of stripe are indicated by white rectangles. The uppermost unit cell is for the (4×1) reconstruction and the lower one is for the (3×1) reconstruction. In the bottom left, a single ridge is labeled A at one end and B at the other. Its morphology changes from (3×1) to (4×1) along its length (image size 30×32 nm^2, sample bias +1.4 V, and tunneling current 0.05 nA).

spots were sometimes visible, usually those closest to the integer order spots. The (1×4) spots are also of very low intensity because only a few coexisting rows of (1×4) are ever situated next to one another.

B. (4×1) reconstruction

Annealing at 1100 °C in UHV for 2 h produces a different reconstruction on the surface. An STM image of the resultant reconstruction is shown in Fig. 4(a). It is made up entirely of stripes running in the $[1\bar{1}0]$ direction. Step edges are far less common than in the case of the (3×1) reconstruction previously shown, and most images show large continuous terraces. When observed, step edges are of irregular shape following no particular crystallographic direc-

tion. Step heights are found to be 0.27 ± 0.02 nm. A single terrace is shown in Fig. 4(a). The stripes are continuous but vary in width. Figure 4(b) shows a region of the reconstruction in greater detail. In this image, two distinct types of stripe are visible. One contains two rows of atoms (labeled A), and the other three (labeled B). Both stripes have a periodicity of 0.57 ± 0.03 nm in the $[1\bar{1}0]$ direction, which is equivalent to one bulk unit cell. The stripes with two rows of atoms have the same width (measured in the [001] direction) as the (3×1) reconstruction reported above and it is likely that they represent this reconstruction. The unit cell is indicated by the lower white rectangle. The stripes with three rows of atoms have a width of 1.64 ± 0.09 nm, which corresponds to four times the bulk unit cell periodicity. This is therefore a (4×1) reconstruction. The unit cell is indicated by the upper white rectangle. The central atomic rows in the STM images of the (4×1) reconstruction contain small defects, whereby an atom does not appear and is instead a dark spot. Along each row, the reconstruction may also change, as the rows can alternate from (3×1) to (4×1) along their length and vice versa. In the bottom left of Fig. 4(b), a single stripe is labeled B at one end and A at the other. This is an example of a stripe that changes from one width to the other along its length. By annealing the surface at higher temperatures, there is an increased prevalence of (4×1) until after annealing at 1175 °C for 2 h a fully (4×1) reconstructed surface is obtained. A LEED pattern of such a surface is shown in Fig. 3(b).

C. (6×1) reconstruction

Annealing at 1275 °C for 2 h in UHV produces another reconstruction, which can be seen in Fig. 5. Figure 5(a) shows a large scale image with a step edge present. The image shows a ridge structure with the ridges following the $[1\bar{1}0]$ direction. The step edge is rough and does not follow the [001] crystallographic direction. It has a height of 0.29 ± 0.01 nm. However, on other images, step edges can be seen to follow the $[1\bar{1}0]$ direction at the edge of a reconstructed ridge. A close-up of the area is shown in Fig. 5(b). The ridges have a width of 2.36 ± 0.07 nm, which is equivalent to six times the bulk unreconstructed lattice parameter in the [001] direction. In Fig. 5(c), the same region is shown but there has been a change in the tip of the STM, which allows more detail to be seen, such as the periodicity in the $[1\bar{1}0]$ direction. Figure 5(d) shows a line scan of the surface in the $[1\bar{1}0]$ direction and indicates that the periodicity is 0.54 ± 0.02 nm. This is equivalent to a bulk unit cell distance in that direction. The ridges thus represent a (6×1) reconstruction. The unit cell is indicated by a white rectangle. This periodicity is confirmed by LEED, which shows a strong (6×1) pattern shown in Fig. 3(c).

In addition, in all parts of Fig. 5, on the lower terrace at the step edge, a region without the (6×1) ridges can be seen. Figures 5(b) and 5(c) show that this region is, in fact, made up of its own stripe structure, but in this case, the stripes run in the [001] direction. By comparing a number of such regions, it is possible to calculate the width of these stripes, which is approximately 1.12 ± 0.03 nm and is equivalent to two times the $[1\bar{1}0]$ bulk unit cell distance. Although it is difficult to see the periodicity in the [001] direction, in some LEED patterns, it is possible to see spots equivalent to a (1×2) pattern [in addition to the spots of the (6×1)]. These spots are very faint as the (1×2) regions are very small and only occur at step edges, but they do suggest that the reconstruction present at the step edges is a (1×2) reconstruction.

D. Auger electron spectroscopy

Additional information can be obtained by using AES. AES was carried out on a surface formed by cleaving a sample in the UHV chamber. This produces a surface that is as close to the $SrTiO_3$ stoichiometry as possible. It is most likely a (100) interface (as that is the lowest energy termination) with equal amounts of SrO and TiO_2 terminations, which overall makes the surface $SrTiO_3$ stoichiometry. The spectrum for the cleaved surface is shown in Fig. 6 as it represents a typical AES spectrum for $SrTiO_3$. The peaks at 380 and 413 eV (*LMM*) are due to the presence of Ti in the surface region. Likewise, the peaks at 492 and 511 eV (*KLL*) are characteristic of O, and Sr is indicated by peaks at 1644 and 1711 eV (*LMM*). The section between 600 and 1400 eV is as a featureless background, which has a relatively constant gradient and is not affected by the concentrations of the relative ionic species within the surface. The featureless background is taken as a reference, and all spectra are scaled so that their featureless backgrounds overlap and are then normalized so that they have an intensity of 1000 counts at 1100 eV (a point in the center of the featureless background).

The spectra for all the reconstructions observed on the $SrTiO_3$ (110) surface are shown in Fig. 7. The normalized peak heights for the cleaved spectrum represent a stoichiometric surface with relative Sr, Ti, and O concentrations of 1, 1, and 3, respectively. By obtaining the peak heights for the other surfaces and comparing their values to that of the cleaved surface, absolute concentrations of each species in all the reconstructions can be calculated. This gives the results given in Table I.

None of the spectra show any peaks due to Nb. The Nb can be assumed to be at such low concentrations that it cannot be detected and no evidence of surface segregation is seen. All the surfaces are deficient in O, ranging from 2.25 to 2.69. In addition, the Ti peak at 413 eV for all the spectra shows a shoulder on the right hand higher energy side. This is the characteristic shape for a Ti^{4+} Auger peak,[8,14,22] and so all the surfaces have Ti^{4+} as their predominant Ti species. The degassed sample in Table I shows the composition of the surface after introduction to the chamber and initial degassing, but before any major surface treatments. This degassed surface is Ti enriched and slightly Sr deficient, although by an insignificant amount. The lower temperature anneal, which produces the (3×1) reconstruction, causes a reduction in the amount of Ti and O and almost no change in Sr relative to the starting point of the as-introduced, degassed surface. This leaves the Sr and Ti levels in the (3×1) reconstruction as close to those of stoichiometry. O, however, has been decreased to 2.25, suggesting that this is an O deficient

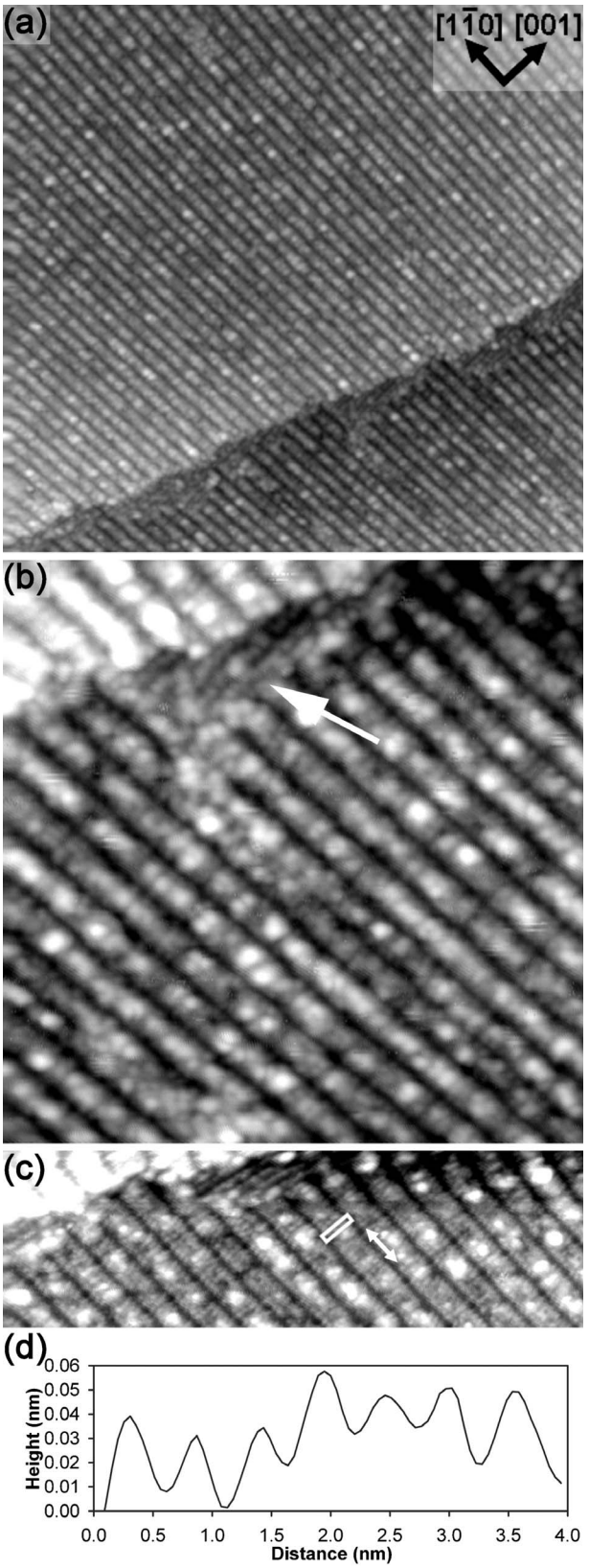

FIG. 5. STM images of the (6×1) reconstruction. (a) An STM image of a terrace of (6×1) surface with a step edge shown. The (6×1) stripes have no noticeable $[1\bar{1}0]$ periodicity. Some regions on the lower terrace close to the step edge appear not to have the ridge structure (image size 100×95 nm^2, sample bias +1.0 V, and tunneling current 0.1 nA). (b) A more detailed image of the same step edge as shown in part (a). Close to the step edge, there is a region of different morphology with stripes running in the [001] direction, as indicated by an arrow. This is a region of (1×2) reconstruction and always forms adjacent to step edges on the lower terrace (image size 36×36 nm^2, sample bias +1.0 V, and tunneling current 0.1 nA). (c) An STM image of the same region as at the top of (b). There has been a change of tip and the periodicity in the $[1\bar{1}0]$ direction can now be seen, confirming it to be the same as the bulk unit cell periodicity in this direction. The unit cell of the (6×1) reconstruction is indicated by a white rectangle (image size 36×13 nm^2, sample bias +1.0 V, and tunneling current 0.1 nA). (d) Line scan for the white double headed arrow in the $[1\bar{1}0]$ direction in part (c). The periodicity is equivalent to the bulk periodicity in this direction (0.55 nm).

surface. The (4×1) surface, which was annealed at 1100 °C, has a higher O concentration at 2.69 and also an above stoichiometric level of Ti (1.22) and a slightly deficient level of Sr. Annealing at this temperature has caused Ti to become enriched at the surface and also for O to have become more enriched in comparison to the degassed surface (although less than that of stoichiometry). The anneal therefore causes an enrichment of TiO_2 at the surface. By contrast, the (6×1) reconstruction has a lower Ti concentration placing it just below stoichiometric levels, and Sr is slightly

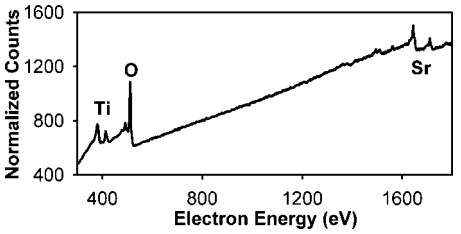

FIG. 6. An Auger spectrum for a $SrTiO_3$ surface produced by cleaving a sample in UHV. This shows the typical features for $SrTiO_3$. The O, Ti, and Sr peaks are indicated. The flat region between 600 and 1400 eV is the featureless background, which is used for normalization. The AES spectra are normalized to a midpoint on that featureless background of 1000 counts at 1100 eV.

enriched in comparison to both stoichiometry and the as-introduced degassed sample. It is therefore likely that the (6×1) has formed by an enrichment of SrO at the surface.

IV. DISCUSSION

The surfaces in this paper mostly show reconstructions where there is a single bulk unit cell periodicity in the $[1\bar{1}0]$ direction and with periodicities of multiples of the bulk unit cell in the [001] direction. These are the (3×1), (4×1), and (6×1) reconstructions. This result is not as expected. One of the easiest ways for a polar surface to reconstruct is for microfaceting to occur, whereby small terraces of nonpolar terminations occur out of plane from the Miller index of the overall surface. On a polar (110) surface, where the (100) surface is nonpolar (as is the case with $SrTiO_3$), microfaceting can be achieved by a concertina of ridges with sides of (100) termination, as shown in Fig. 8(a). If this were to occur, then the periodicity of the overall surface would become greater in the $[1\bar{1}0]$ direction and stay constant in the [001] direction relative to the bulk termination. This is the opposite of what is reported in this paper. Thus, microfaceting into (100) surfaces can be discounted as the reason for the production of the reconstructions. Microfaceting into (111) surfaces is a possibility as this would increase the periodicity in the [001] direction, as shown in Fig. 8(b), but it is unlikely as the (111) surface is also polar. Faceting a (110) surface into (111) planes produces parallel trenches in the $[1\bar{1}0]$ direction with a depth of $w/\sqrt{8}$ when the trench has a width of w. The periodicities of the (3×1), (4×1), and (6×1) reconstructions in the [001] direction are 1.17, 1.56, and 2.34 nm, re-

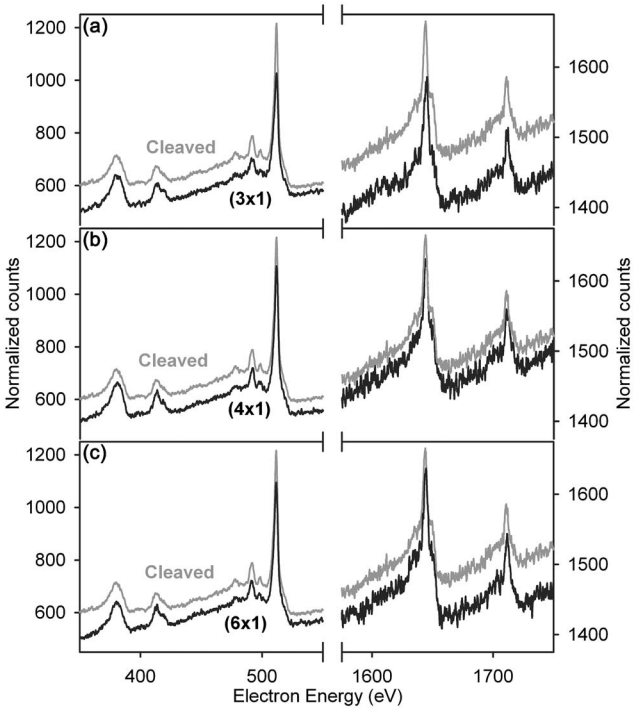

FIG. 7. Auger spectra of the reconstructions on the $SrTiO_3$ (110) surfaces. (a) Spectra of the (3×1) surface (black) and the cleaved stoichiometric surface (gray). The Ti and Sr peaks of the cleaved and reconstructed samples are similar, but the O peak is much smaller for (3×1) than for the cleaved sample. (b) The spectrum of the (4×1) surface (black). The Ti peak is larger for the reconstructed surface than for the cleaved surface (gray). The Sr peaks are similar, but the O peak is smaller for the (4×1) reconstruction. (c) The spectrum for the (6×1) reconstruction (black). The O concentration for the (6×1) is deficient, and the Ti is similar to that of stoichiometry (gray), but the Sr peak for the reconstructed surface is larger than that for stoichiometry.

TABLE I. The concentrations of different species in each of the $SrTiO_3$ (110) reconstructions. The cleaved surface represents stoichiometry, and the degassed surface the as-introduced polished sample. All the surfaces are O deficient, but while the (3×1) surface is close to stoichiometric in Sr and Ti, the (4×1) surface is Ti enriched and the (6×1) surface is Sr enriched. The error associated with the Ti values is ±7%, for Sr it is ±5%, and for O it is ±2%.

	O	Ti	Sr
Cleaved (normalized)	3.00	1.00	1.00
Degassed	2.54	1.33	0.91
(3×1)	2.25	1.04	0.96
(4×1)	2.69	1.22	0.91
(6×1)	2.61	0.95	1.12

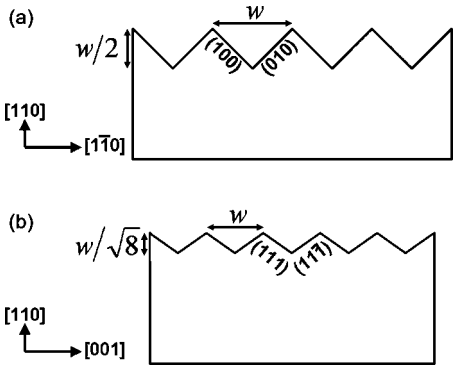

FIG. 8. Schematic of faceting of the (110) surface showing the surface viewed from the side. (a) Faceting to form (001) planes causes parallel trenches in the [001] direction. These trenches have a depth of half their width. (b) Faceting into (111) planes causes parallel trenches to form in the $[1\bar{1}0]$ direction. The trenches have a depth of $w/\sqrt{8}$ assuming that they have a width w.

spectively. For (111) faceting to occur, corrugation heights of 0.41, 0.55, and 0.83 nm would be necessary, respectively, for the (3×1), (4×1), and (6×1) reconstructions. The measured corrugation heights are 0.06, 0.16, and 0.21 nm for the (3×1), (4×1), and (6×1) reconstructions. These are not nearly large enough to suggest that faceting into (111) surface planes is the cause of any of these reconstructions. Likewise, the (1×4) and (1×2) reconstructions have measured corrugation heights of 0.18 and 0.11 nm, respectively [although as the (1×2) domains were very small, this is difficult to measure]. Faceting into (001) planes causes parallel trenches in the [001] direction with a depth of half their width, and so for faceting into (001) planes to be the cause of these reconstructions, corrugations of 1.10 and 0.55 nm would be observed. This again is far larger than that observed and so faceting can be discounted.

All the surfaces have the same starting point, being the degassed, as-introduced polished surface. Thus, the only factor influencing the final reconstruction is the annealing temperature and time. The lowest temperature annealed sample gave the (3×1) reconstruction with some areas of (1×4) near step edges. This structure has near stoichiometric Sr and Ti but is O deficient in the surface region. Given that the majority of the surface is covered in (3×1), this composition is most likely due to the influence of the (3×1) reconstruction. As the (3×1) surface cannot be caused by microfaceting, it must represent a surface reconstruction, which appears to be stabilized by the loss of O. In addition, the (1×4) reconstruction appears to form preferentially at step edges in the [001] direction, usually along the upper terrace. Trying slightly lower or higher temperature anneals does not cause (1×4) to appear alone, and it does not appear that either (3×1) or (1×4) appears first and then is superseded by the other with higher temperature annealing. It is possible that step edges following the [001] direction are unfavorable for the (3×1) reconstruction due to the anisotropy of the crystallographic directions on the $SrTiO_3$ (110) surface and the fact that the ridges of the (3×1) surface are perpendicular to the [001] direction. It is likely that the (1×4) reconstruction represents a metastable kinetic phase, which may stabilize the [001] the step edges, or are themselves stabilized by the step edge, or the stoichiometry at the edge. However, the (3×1) reconstruction always dominates the surface. Since step edges along the [001] and $[1\bar{1}0]$ directions are always decorated by (1×4) and (3×1) reconstructions respectively, the step edges are always in line with a ridge, and so straight. The (1×4) periodicity is not due to faceting as the surface does not appear to have enough of a corrugation. Brunen *et al.*[17] have previously reported a (3×4) reconstruction, which was formed under similar conditions. This was based on LEED results very similar to ours and without any corroborating STM images. They interpreted their LEED pattern as (3×4) with a large number of missing spots. However, their result can be more readily interpreted as a $(3\times1)/(1\times4)$ coreconstruction, which would be in agreement with our results. We thus believe that the surface reported by Brunen *et al.* as a (3×4) is, in fact, the same as our $(3\times1)/(1\times4)$ coreconstruction and that, thanks to the periodicities visible in our STM images, can now be confirmed as such.

The (4×1) reconstruction occurs at higher temperature anneals, and while its Sr levels are similar to those of the (3×1), it has higher Ti and O concentrations. Its Ti concentration is, in fact, greater than stoichiometry, although O is still deficient with respect to stoichiometry. It is likely that the (4×1) has formed by the increase of TiO_2 at the surface via segregation from the bulk. The higher temperature allows this to happen as it will increase the mobility of Ti and O. O is known to be mobile in $SrTiO_3$, as annealing causes O vacancies to appear in the bulk. At higher temperatures, Ti can become mobile, as has been shown in both $SrTiO_3$ (111) (Refs. 14 and 15) and $SrTiO_3$ (100).[4,5,23] Also, in the STM images, both (3×1) and (4×1) are shown to coexist. The (3×1) reconstruction appears to be the same as that imaged with the (1×4) reconstruction after lower temperature anneals. The images show that a single ridge on the surface can transform from (3×1) to (4×1) as you travel down its length, suggesting that the (4×1) forms out of the (3×1). It is likely that on increasing annealing temperature, the surface first forms a (3×1) reconstruction, and then as the temperature increases, this transforms to (4×1). The (4×1) reconstruction appears in the images as three rows of atoms, and the (3×1) surface as two rows. It is possible that this extra row represents TiO_2 enrichment, as the (4×1) reconstruction shows an increase in Ti and O but a decrease in Sr relative to the (3×1) surface. In addition, the (4×1) has step edges which do not follow strict crystallographic directions and these are not decorated by (1×4), which appears to no longer be stable on this higher temperature annealed surface. However, as (4×1) and (3×1) can form together on the same surface, it is likely that they are related to one another and that they have similar structures and energies.

The (6×1) reconstruction represents a slightly Sr enriched phase. It forms at the highest temperature of all the reconstructions. At this temperature, it appears that the Sr becomes mobile and itself segregates to the surface. The (6×1) reconstruction has a definite ridge structure, and it is far harder to image the periodicity in the $[1\bar{1}0]$ direction than for the other reconstructions. Again, the step edges do not follow the [001] direction (although step edges following the $[1\bar{1}0]$ direction parallel to the ridges are observed). The rough step edges are again decorated with a different reconstruction. The lower terrace at the step edge has a (1×2) reconstruction close to it. The (1×2) reconstruction is always found on the lower terrace adjacent to a step edge. This is not as common as the (1×4) on the (3×1) surface nor does it affect the random orientation of the step edge. The (1×2) reconstruction is likely to represent a metastable kinetic phase, which is stabilized by the proximity to the step edge. As the (1×2) reconstruction has stripes following the [001] direction, it is possible that this surface is microfaceted. It has been modeled that the (1×2) surface can stabilize the $SrTiO_3$ (110) surface,[24] and it has been observed on other occasions.[19,20]

All the surfaces observed in this paper are not able to be imaged at sample biases close to 0 V. STM imaging is not possible at biases of less than +0.5 V nor at negative bias. This shows that the surface reconstructions are not conducting, i.e., the Fermi level is situated deep within the band gap. The AES spectra of all the surfaces indicate reduced oxygen

levels compared to stoichiometry. We would therefore expect the presence of some Ti in a lower oxidation state than Ti^{4+}. TiO is a metallic material, and if metallic states were observed, then this would suggest that Ti^{2+} is present at the surface. As this is not the case, we can discount the possibility of Ti^{2+} ions in the surface region. Insulating character is more likely for Ti^{4+} and Ti^{3+}. The characteristic peak shape between 406 and 426 eV in the AES analysis matched that seen for other Ti^{4+} rich surfaces.[8,14,15] This suggests that it is likely that the predominant Ti species present in the surface region is Ti^{4+} with some Ti^{3+} also present.

The step edges on the surface were always equivalent to the distance between two similar SrTiO planes or O_2 planes in the $\langle 110 \rangle$ direction. This distance is known as the d_{110} lattice parameter (0.28 nm) and shows that the reconstructions form out of only one of these planes. Our definition of the d_{110} lattice parameter should not be confused with the periodicity of the bulk crystal in the [110] direction, which has double the value (0.56 nm). If step edges with a height of 0.5 d_{110} were to form, it would show that one surface represented a reconstruction of the O_2 plane, and the other a reconstruction of the SrTiO plane. However, this has not been observed.

Finally, we can also discount the possibility of Nb having an effect on the surface structure. The AES analysis showed there to be no detectable level of Nb at the surface. Surface enrichment of Nb has not occurred and, therefore, the surfaces cannot be a niobate or even an Nb stabilized strontium titanate phase. The Nb does allow the sample to become conducting. Given that $SrTiO_3$ (110) is a polar surface, this could allow a simple mechanism for the rearrangement of charge density in the sample, preventing the surface induced polarity. By providing a separate mechanism for the prevention of polarity, it may mean that a surface phase that would have formed for this purpose on pure $SrTiO_3$ will now not form, and a different lower energy surface will be able to form on the Nb doped sample. However, this is unlikely as the Nb doping merely mimics the effect of reduction. On annealing in O poor environments, O vacancies are formed in the bulk, which act in a similar way to doping the sample *n*-type. Thus, the same conducting properties as provided by Nb doping could be produced simply by severe reduction and would be possible on pure $SrTiO_3$ samples.

V. CONCLUSIONS

$SrTiO_3$ (110) produces a number of $(n \times 1)$ reconstructions when annealed in UHV. Increasing the temperature changes the reconstruction formed, starting initially as a (3×1) reconstruction, and then changing into a (4×1), and, finally, a (6×1) surface. All the surfaces show a deficiency in O, but this is most pronounced in the (3×1) reconstruction. The (3×1) reconstruction coexists with regions of (1×4), which usually decorate the step edges in the [001] direction. The (6×1) reconstruction contains small amounts of (1×2) reconstruction on the lower terrace adjoining step edges. The (4×1) reconstruction shows Ti enrichment, and the (6×1) surface shows Sr enrichment. The enrichment of both of these species is not as pronounced as seen on the $SrTiO_3$ (111) and (100) surfaces. Surprisingly, none of the surface treatments result in microfaceting, which had previously been proposed as a likely surface stabilization mechanism.

ACKNOWLEDGMENTS

The authors would like to thank D. T. Newell for allowing the reproduction of his UHV cleaved Auger data and Chris Spencer (JEOL UK) for his technical support. We are also grateful to the EPSRC for funding.

*martin.castell@materials.ox.ac.uk

[1] D. S. Deak, F. Silly, D. T. Newell, and M. R. Castell, J. Phys. Chem. B **110**, 9246 (2006).
[2] M. R. Castell, Surf. Sci. **516**, 33 (2002).
[3] M. R. Castell, Surf. Sci. **505**, 1 (2002).
[4] N. Erdman, L. D. Marks, K. R. Poeppelmeier, M. Asta, O. Warschkow, and D. E. Ellis, J. Am. Chem. Soc. **125**, 10050 (2003).
[5] N. Erdman, K. R. Poeppelmeier, M. Asta, O. Warschkow, D. E. Ellis, and L. D. Marks, Nature (London) **419**, 55 (2002).
[6] Q. D. Jiang and J. Zegenhagen, Surf. Sci. **425**, 343 (1999).
[7] Q. Jiang and J. Zegenhagen, Surf. Sci. **367**, L42 (1996).
[8] D. T. Newell, A. Harrison, F. Silly, and M. R. Castell, Phys. Rev. B **75**, 205429 (2007).
[9] T. Kubo and H. Nozoye, Phys. Rev. Lett. **86**, 1801 (2001).
[10] H. Tanaka, T. Matsumoto, T. Kawai, and S. Kawai, Jpn. J. Appl. Phys., Part 1 **32**, 1405 (1993).
[11] P. W. Tasker, J. Phys. C **12**, 4977 (1979).
[12] C. Noguera, J. Phys.: Condens. Matter **12**, R367 (2000).
[13] J. Goniakowski, F. Finocchi, and C. Noguera, Rep. Prog. Phys. **71**, 016501 (2008).
[14] B. C. Russell and M. R. Castell, J. Phys. Chem. C **112**, 6538 (2008).
[15] B. C. Russell and M. R. Castell, Phys. Rev. B **75**, 155433 (2007).
[16] E. Heifets, W. A. Goddard, E. A. Kotomin, R. I. Eglitis, and G. Borstel, Phys. Rev. B **69**, 035408 (2004).
[17] J. Brunen and J. Zegenhagen, Surf. Sci. **389**, 349 (1997).
[18] H. Bando, Y. Aiura, Y. Haruyama, T. Shimizu, and Y. Nishihara, J. Vac. Sci. Technol. B **13**, 1150 (1995).
[19] A. Gunhold, L. Beuermann, V. Kempter, W. Maus-Friedrichs, K. Gömann, and G. Borchardt, Surf. Sci. **566-568**, 105 (2004).
[20] A. Gunhold, L. Beuermann, V. Kempter, W. Maus-Friedrichs, K. Gömann, G. Borchardt, S. Piskunov, E. A. Kotomin, and S. Dorfman, Surf. Interface Anal. **35**, 998 (2003).
[21] J. A. Noland, Phys. Rev. **94**, 724 (1954).
[22] W. J. Lo and G. A. Somorjai, Phys. Rev. B **17**, 4942 (1978).
[23] N. Erdman and L. D. Marks, Surf. Sci. **526**, 107 (2003).
[24] F. Bottin, F. Finocchi, and C. Noguera, Surf. Sci. **574**, 65 (2005).
[25] K. Hermann, *in Computer Code LEEDPAT* (Fritz-Haber-Institut, Berlin, 2006).